IL NUOVO CIMENTO **46 C** (2023) 149
DOI 10.1393/ncc/i2023-23149-y

COMMUNICATIONS: SIF Congress 2022

Dual-comb laser enables broadband detection of optical anisotropies

F. CALLEGARI([1])([2])(*), A. NUSSBAUM-LAPPING([3]), B. WILLENBERG([3]), J. PUPEIKIS([3]), A. ZUNINO([4]), A. LE GRATIET([5]), P. BIANCHINI([1]), A. DIASPRO([1])([2]), C. R. PHILLIPS([3]) and U. KELLER([3])

([1]) *Nanoscopy and NIC@IIT, Istituto Italiano di Tecnologia (IIT) - 16152 Genova, Italy*
([2]) *Department of Physics, University of Genova - 16152 Genova, Italy*
([3]) *Department of Physics, Institute for Quantum Electronics, ETH Zurich - 8093 Zurich, Switzerland*
([4]) *Molecular Microscopy and Spectroscopy, Istituto Italiano di Tecnologia (IIT) 16152 Genova, Italy*
([5]) *Université de Rennes, CNRS, Institut FOTON - UMR 6082 Lannion, France*

received 31 January 2023

Summary. — The measurement of optical anisotropies is widely employed in many application fields, such as material and biomedical sciences. Such spectroscopic method monitors the polarization state alterations after the interaction between matter and different states of polarized light. Here, we use a newly developed single-cavity dual-comb laser to demonstrate proof-of-principle polarization-resolved measurements. We detect the signals resulting from the heterodyne mixing of the two combs. The interferograms encode the information about the polarimetric properties of samples at kHz rate. Our results complement earlier work with similar single-cavity dual-comb lasers demonstrating pump-probe sampling, and pave the way for a new platform for multimodal sensing.

1. – Introduction

Single-cavity dual-comb lasers (DCLs) are sources where a pair of optical frequency combs (OFCs) is generated from the same cavity with a slightly different comb line spacing. In the time domain, this corresponds to a pair of ultrashort pulse trains with a slightly different repetition rate. Single-cavity dual-comb generation is achieved by having the two beams travel through different optical paths in the cavity by introducing a multiplexing element [1, 2]. DCL allows the characterization of spectral fingerprints

(*) E-mail: fabio.callegari@iit.it

in the optical range by measuring radio frequency (RF) signals, greatly simplifying the optical setup. For such reason, DCLs have found many applications in high-precision spectroscopy [3, 4], laser ranging [5, 6], pump-probe spectroscopy [7], and microscopy [8]. Also, polarization-resolved spectroscopy methods based on DCLs have been developed, but none of them relies on a compact single-cavity dual-comb laser. The optical setup requires the synchronization of two mode-locked lasers using complex and bulky electronic devices [9].

We developed a single-cavity DCL whose properties have been already described in [10]. Here we provide the theoretical model and experimental method to probe optical anisotropies of samples by analyzing the heterodyne mixing of the two combs emitted by the same device. We used the Stokes-Mueller formalism to model the polarization evolution within our setup [11]. This technique can be used to implement polarization measurements in an optical setup where the DCL source inherently modulates the polarization state. This feature simplifies the architecture of the optical setup, since it does not exploit external devices for polarization generation. Moreover, this method allows broadband characterization of optical anisotropies, since the RF interferograms bring the fingerprint of the whole DCL output bandwidth.

2. – Polarization-resolved ultrafast interferometry

The properties and characterization of our single-cavity DCL have been already reported in [10]. To quickly summarize them, it emits two spatially separated, co-polarized twin beams at 1057 nm with 1 GHz repetition rate (f_r), each carrying 3 W average power. For the experiments presented in this paper, the laser was in a similar configuration with slightly different performances. The main differences are the longer pulse duration (100 fs) and the presence of a dip in the spectrum tail around 1068 nm. A minor modification to the laser architecture allowed to clean up spectra, obtain shorter pulses (shorter than 80 fs), and increase power extraction (> 3 W), as reported in [10]. The repetition rate difference ($\Delta f_r = f_{r1} - f_{r2}$) between the two combs can be tuned up to 27 kHz by adjusting the vertical position of an intracavity biprism. We redirect the two co-polarized beams emitted by our DCL through a stage used to shape their polarizations and overlap them. We set them in two linear and orthogonal states by using a half-wave plate (HWP) placed in each arm of the setup. We combine the two beams through a polarizing beam splitter (PBS) whose main axes are aligned with the input cross-polarized states.

Then we rotated the combs polarizations at $\pm 45°$ with respect to the PBS axes by using another HWP placed after it. Each pair of comb lines with the same index n in the diagonal-antidiagonal ($A - D$, $\pm 45°$) state has a Stokes vector described as follows:

(1)
$$\vec{S}_{in,n} = \begin{pmatrix} s_{1,n} \\ s_{2,n} \\ s_{3,n} \\ s_{4,n} \end{pmatrix} = \begin{pmatrix} |E^2_{D,n}(t)| + |E^2_{A,n}(t)| \\ |E^2_{D,n}(t)| - |E^2_{A,n}(t)| \\ E_{D,n}(t)E^*_{A,n}(t) + E^*_{D,n}(t)E_{A,n}(t) \\ j(E_{D,n}(t)E^*_{A,n}(t) - E^*_{D,n}(t)E_{A,n}(t)) \end{pmatrix} \propto \begin{pmatrix} 1 \\ \cos(n\Delta\omega_r t) \\ 0 \\ \sin(n\Delta\omega_r t) \end{pmatrix},$$

where $E_{D,n}(t), E_{A,n}(t)$ terms denote the electric fields associated with the cross-polarized modes. The oscillating components at $n\Delta\omega_r = n2\pi\Delta f_r$ describe a time-varying polarization state that is bounded to the repetition rate difference of the two combs: here we set $\Delta f_r \approx 2$ kHz. So, we have assumed $\Delta f_r \ll f_r$ and no carrier-envelope offset frequency difference for simplicity. Then, the sample impresses its optical anisotropies

Fig. 1. – (a) Comb 1 (red) and comb 2 (blue) with their respective polarization states (red and blue double-sided arrows). (b) A typical interferogram recorded after the Wollaston prism and the associated Fourier-transformed spectrum in the RF range.

on light, and a Wollaston prism used as a Polarization State Analyzer (PSA) splits the altered polarization components into two parts. The two PSA outputs are detected by fast photodiodes (DET01CFC, Thorlabs, USA, PD_H, and PD_V in fig. 1). The following matrix product $\vec{S}_{out,k} = [M_{PSA,k}] \cdot [M_{sample}] \cdot \vec{S}_{DCL}$ describes the output polarization states of the system. Here, $[M_{PSA,k}]$ is the Mueller matrix of the PSA filtering the horizontal ($k = H$, 0°) and vertical ($k = V$, 90°) polarization state in the two separate outputs. Each photodiode detects an interferogram train rising from the mixing of the two combs. The 45° angle between the cross-polarized state and the PSA axes is needed to generate the interferograms also when isotropic material is present as a sample. We analyze the associated photocurrents $i_k(t)$, proportional to the first element of $\vec{S}_{out,k}$. The self-mixing signal in the range $[0, f_r/2]$ is the sum of n beating signals as

$$i_{k,n}(t) \propto a_{k,n} + b_{k,n} \cdot \cos(n\Delta\omega_r t) + c_{k,n} \cdot \sin(n\Delta\omega_r t). \tag{2}$$

Amplitude coefficients $a_{k,n}, b_{k,n}, c_{k,n}$ in eq. (2) are linear combinations of the Mueller matrix elements that describe the sample response. Thus, we perform the Fourier transform on the detected interferograms. Since the RF spectrum is a down-converted replica of the spectral alterations in the near-infrared range, we can map the optical anisotropies within the DCL bandwidth.

3. – Broadband characterizations of optical anisotropies

Our measurements have been performed by recording the photocurrent variations while rotating a polarization optics with respect to its azimuthal angle. As a reference sample (indicated in green in fig. 1) we used a zero-order quarter waveplate (WPQ05M-1053, Thorlabs, USA). A pair of signals $i_H(t)$, $i_V(t)$ have been detected for each angle, with an angular step of 10°. Then, we Fourier-transformed the associated photocurrents and we used their amplitude and phase coefficients to calculate the Mueller elements. When no sample alters the light polarizations, the interferograms are associated with an exact replica of the optical spectra of the two combs in the RF range. If the sample contains any optical anisotropy, the light polarization is modified and the Fourier-transformed interferograms are altered accordingly.

Each plot in fig. 2 represents the spectral map of a different Mueller coefficient. The RF band between 135 and 160 MHz correspond to the DCL output spectra with 12 nm full width half maximum. The low laser power in the spectral dip around 155 MHz hinders a proper identification of the Mueller elements at that frequency.

The m_{11} element is used for normalization, since it corresponds to the total collected light. Mueller coefficients associated with dichroism (m_{12}, m_{21}, m_{14}) are null.

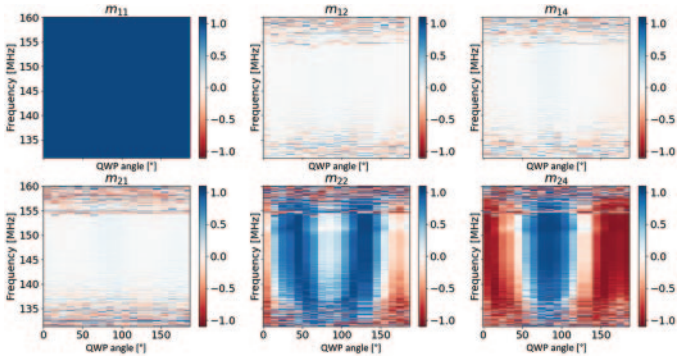

Fig. 2. – Spectral maps of the Mueller coefficients as a function of the azimuthal angle of the quarter-wave plate.

Conversely, those associated with depolarization and linear birefringence (m_{22}, m_{24}) exhibit the sinusoidal variation as expected with a birefringent waveplate.

4. – Conclusion

DCLs are crucial tools for a variety of applications requiring fast and precise spectral measurements. Our method employs a fast modulation of the polarization state without using external active devices to measure the optical anisotropies of samples. This technique can be applied to any DCL source, and its performance can be improved by combining this approach with the coherent averaging procedure described in [10]. Moreover, the dual-comb spectra can be broadened and shifted using a nonlinear optical conversion stage. Both spectral and timing properties of DCL emission allow the implementation of several spectroscopic investigations simplifying the structure of the measurement setup. Therefore, DCLs can be used to develop a multimodal sensing platform combining different techniques to probe several physical properties of samples.

REFERENCES

[1] Liao R. *et al.*, *J. Phys.: Photon.*, **2** (2020) 042006.
[2] Link S. M. *et al.*, *Opt. Express*, **23** (2015) 5521.
[3] Schiller S., *Opt. Lett.*, **27** (2002) 766.
[4] Coddington I. *et al.*, *Optica*, **3** (2016) 414.
[5] Camenzind S. L. *et al.*, *Opt. Express*, **30** (2022) 37245.
[6] Coddington I. *et al.*, *Nat. Photon.*, **3** (2009) 351.
[7] Pupeikis J. *et al.*, *Opt. Express*, **29** (2021) 35735.
[8] Mizuno T. *et al.*, *Sci. Adv.*, **7** (2021) 1.
[9] Sumihara K. A. *et al.*, *J. Opt. Soc. Am. B*, **34** (2017) 154.
[10] Phillips C. R. *et al.*, *Opt. Express*, **31** (2023) 7103.
[11] Fujiwara H., *Spectroscopic Ellipsometry* (Wiley) 2007, pp. 1–369.